Lecture Notes in Physics, (edited by S. M. Deshpande, S. S. Desai, R. Narasimha), No. 453, pp. 372-377, Springer-Verlag, Berlin, (1995).

Transonic Inviscid/Turbulent Airfoil Flow Simulations Using a Pressure Based Method with High Order Schemes

Gang Zhou, Lars Davidson and Erik Olsson
Thermo and Fluid Dynamics, Chalmers University of Technology,
S-412 96 Gothenburg, Sweden

This paper presents computations of transonic aerodynamic flow simulations using a pressure-based Euler/Navier-Stokes solver. In this work emphasis is focused on the implementation of higher-order schemes such as QUICK, LUDS and MUSCL. A new scheme CHARM is proposed for convection approximation. Inviscid flow simulations are carried out for the airfoil NACA 0012. The CHARM scheme gives better resolution for the present inviscid case. The turbulent flow computations are carried out for the airfoil RAE 2822. Good results were obtained using QUICK scheme for mean motion equation combined with the MUSCL scheme for k and ϵ equations. No unphysical oscillations were observed. The results also show that the second-order and third-order schemes yielded a comparable accuracy compared with the experimental data.

1 Introduction

Traditionally most transonic aerodynamic flow simulations are carried out by using density based methods (or time-marching methods as often called) in which density is used as a primary variable in the continuity equation, while pressure is extracted from the equation of state. Recently there are a few successful computations[1–4] obtained from the pressure-based method which use pressure as the dependent variable for transonic airfoil flow, which is the most challenging case for the demonstration of how well a pressure-based method can resolve physical discontinuities such as external shocks. The previous works[1,3,4] have shown that an advanced pressure-based method has a resolution comparable to, or better than, the traditional time-marching methods. This paper presents computations of both inviscid and turbulent transonic aerodynamic flow using the proposed pressure-based method in Refs. (1,3,4). Higher-order schemes such as QUICK,[5] LUDS, MUSCL[6] and a newly proposed bounded third-order scheme CHARM[7] are used.

In recent years, many high resolution schemes have been proposed and investigated like unbounded QUICK[5], bounded SMART[8] and SHARP[9]. A piecewise linear blending function is used in SMART and a non-linear one in SHARP in combination with variable normalization to make them bounded. All these schemes are of third-order accuracy. To simplify the algorithm involved in third-order scheme (causing insignifcant loss of accuracy), many second-order accuracy schemes have been proposed, like HLPA[10] and TVD MUSCL. The scheme HLPA (Hybrid Linear / Parabolic Approximation) uses a second order polynomial in the monotonic region of the normalized variable diagram (NVD). This method is similar to van Leer's scheme[11]. The TVD MUSCL scheme, which adopts the TVD flux limiter concept and variable normalization approach, employs a combination of a central differencing scheme (CDS) and a second linear upwind differencing scheme (LUDS). The result is a bounded second-order approximation which can be used for all convection transport variables including k and ϵ. These two schemes are one order of accuracy less than QUICK in terms of the Taylor series truncation error. However, they are unconditionally bounded, simple to implement in many applications and yield results with no substantial difference in accuracy compared to third-order scheme. Combining the respective advantages of the higher order accuracy of third-order schemes and that of boundedness, algorithmic simplicity of a second-order scheme, on the basis of the principle of *Leonard*'s NVD characteristic, one can design a new generation of high-order schemes. The CHARM (Cubic-parabolic High Accuracy Resolution Method), presented in this work is a new unconditionally bounded scheme with essentially third-order accuracy.

Along the mutual influence on the development of high order schemes between pressure-based methods and time-marching methods, many efforts[1-4] also focus on the advance of pressure-based method to external transonic flow simulations especially with the shocks. *Leonard*[9] has shown the similarities between variable normalization approach and the flux limiter which is normally adopted in time-marching methods. More recently, *Zhou and Davidson*[3] have shown the numerical dissipation models used in pressure-based method and in density-based methods have similar properties. The similarities between these two methods indicated that these two methods should have comparable abilities to simulate highly convective flows in computational fluid dynamics.

In this work we use a pressure-based Euler/Navier-Stokes SIMPLE solver in a finite volume frame employing a non-orthogonal collocated arrangement. An implicit artificial dissipation model is used, which consists of second- and fourth-order derivative of pressure in all equations. It was found that two-level filters should be used to adjust second-order dissipation for inviscid flow simulations. For turbulent airfoil flow, however, only one level filter needs to be used. The results have shown a good capability of predicting both internal and external inviscid transonic flows[3] including shock capturing. A $k-\epsilon$ turbulence closure with a near-wall one-equation model is used for the turbulent flow cases. The second-order accuracy scheme MUSCL is adopted for approximating turbulence transport properties. The results of the prediction of the turbulent transonic flow around airfoil RAE 2822 for *case* 6, and *case* 10 of Cook *et al.*[12] show good agreement with experimental data.

2 High accuracy approximation for convection

2.1 Linear schemes

Following *Leonard*'s[9] variable normalization consideration, the face normal velocity at the right-hand face of the central volume (CV) at i can been nondimensionalized in upstream sense as

$$\hat{\Phi}_{i+1/2} = \frac{\Phi_{i+1/2} - \Phi_{i-1}}{\Phi_{i+1} - \Phi_{i-1}}. \tag{1}$$

A general form of second- and third-order linear (in NVD) schemes may be written as

$$\Phi_{i+1/2} = \Phi_i + \frac{1}{4}\left[(1-\kappa)(\Phi_i - \Phi_{i-1}) + (1+\kappa)(\Phi_{i+1} - \Phi_i)\right]. \tag{2}$$

The normalized form of Eq. (2) is

$$\hat{\Phi}_{i+1/2} = \hat{\Phi}_i + \frac{1}{4}\left[(1-\kappa)\hat{\Phi}_i + (1+\kappa)\left(1-\hat{\Phi}_i\right)\right]. \tag{3}$$

Note that, the numerical parameter κ controls the order of scheme. Setting $\kappa = 1$, -1 and 0.5, one gets linear CDS, LUDS and QUICK scheme respectively. Adopting TVD flux limiters, one can get a piece-wise linear MUSCL scheme as follows

$$\hat{\Phi}_{i+1/2} = \begin{cases} \hat{\Phi}_i + \frac{1}{2}\,min\left\{\hat{\Phi}_i, \left(1-\hat{\Phi}_i\right)\right\}, & \frac{\hat{\Phi}_i}{1-\hat{\Phi}_i} > 0, \\ \hat{\Phi}_i, & \frac{\hat{\Phi}_i}{1-\hat{\Phi}_i} \leq 0. \end{cases}$$

This scheme combines the second linear upwind scheme and the central differencing schemes and can be written as follows,

$$\hat{\Phi}_{i+1/2} = \begin{cases} \frac{3}{2}\hat{\Phi}_i, & \hat{\Phi}_i \in [0, 0.5], \\ \frac{1}{2}\left(1+\hat{\Phi}_i\right), & \hat{\Phi}_i \in (0.5, 1], \\ \hat{\Phi}_i, & \hat{\Phi}_i \ni [0,1]. \end{cases}$$

Note that all schemes pass the critical point $Q(0.5, 0.75)$ (see Fig. 1) through which any schemes is at least of second order accuracy. The TVD MUSCL scheme passes the point and then follows the lower border of the second-order region. The scheme HLPA passes the point, but with a non-linear second polynomial function.

2.2 CHARM scheme

As an additional necessary and sufficient condition, as pointed out by *Leonard*[9], any approximation function passing Q with a slope 0.75 is of third-order accuracy. The scheme QUICK meets the condition, and it reads

$$\hat{\Phi}_{i+1/2} = \frac{3}{4}\hat{\Phi}_i + \frac{3}{8}. \tag{4}$$

The scheme SHARP[8] uses an exponential upwinding function which is tangent to the QUICK line at point Q. Obviously it is third-order accurate. Nevertheless, the exponential upwinding is more expensive than a polynomial. Our object is to replace the exponential upwinding function with a third-order polynomial which is tangent to the QUICK scheme at the point Q point. A <u>C</u>ubic-parabolic <u>H</u>igh <u>A</u>ccuracy <u>R</u>esolution <u>M</u>ethod, CHARM, is designed as follows

$$\hat{\Phi}_{i+1/2} = \begin{cases} \hat{\Phi}_i^3 - 2.5\hat{\Phi}_i^2 + 2.5\hat{\Phi}_i, & \hat{\Phi}_i \in [0,1], \\ \hat{\Phi}_i, & \hat{\Phi}_i \ni [0,1]. \end{cases}$$

Figure 1 shows the characteristic of CHARM. In terms of non-normalized variables, the cubic-parabolic part of the above equation has the form

$$\Phi_{i+1/2} = \Phi_i + \kappa\left(\Phi_i - \Phi_{i-1}\right)\left(\hat{\Phi}_i^2 - 2.5\hat{\Phi}_i + 1.5\right) \tag{5}$$

with the parameter κ

$$\kappa = \begin{cases} 1, & |\hat{\Phi}_i - 1.5| \leq 0.5, \\ 0, & \hat{\Phi}_i \ni [0,1]. \end{cases}$$

It can be shown that the convective stability is satisfied. A numerical negative feedback mechanism which reduces the convective influx, $\mathbf{F_i}$, when Φ_i increases, or *vice versa*, ensures the convergency. Assuming one-dimension flow, for example, with a constant convecting velocity ($U = U_0$), we have, for $\hat{\Phi} \in [0,1]$, that

$$\frac{\partial \mathbf{F_i}}{\partial \Phi_i} = U_0 \frac{\partial \left(\Phi_{i-1/2} - \Phi_{i+1/2}\right)}{\partial \Phi_i} = U_0 \left(-2\hat{\Phi}_{i-1}^3 + 2.5\hat{\Phi}_{i-1}^2 - 3\hat{\Phi}_i^2 + 2.5\hat{\Phi}_i - 2.5\right) < 0. \quad (6)$$

It is obvious that Eq. (5) represents a first-order upwind formulation with a third-order correction, which is implemented as explicit *sources/sink* terms in an iterative sequence leading to a steady-state solution.

3 Numerical Procedure

The SIMPLE procedure is used to achieve steady solution for both inviscid and turbulent flow cases. All the govering equations can be cast into a standard transport equation for a general dependent variable Φ, in Cartesian coordinates, as

$$\frac{\partial}{\partial t}(\Phi) + \frac{\partial}{\partial x_i}(U_i \Phi) = \frac{\partial}{\partial x_i}\left[\Gamma_\Phi \frac{\partial}{\partial x_i}\left(\frac{\Phi}{\rho}\right)\right] + S^\Phi \quad (7)$$

where Φ can be the Cartesian mass flux components, pressure correction, ρk or $\rho\epsilon$, Γ_Φ is the effective diffusivity, and S_Φ denotes source per unit volume for the dependent variables Φ. In the inviscid case $\Gamma_\Phi = 0$. Integrating Eq. (7) over all the control volumes, by using the Gaussian theorem, we get the following discretized equation

$$\left(\Phi - \Phi^0\right)\frac{\delta v}{\triangle t} + \sum_m (\mathbf{F} \bullet \mathbf{A}) - \sum_m (\Gamma_\Phi \nabla \Phi \bullet \mathbf{A}) = S_\Phi \delta v \quad (8)$$

where $\mathbf{F}$ is the flux tensor, δv is the volume of the cell, m refer to each face $\mathbf{A}$ of the control volume, and Φ^0 is value at previous time level. The discretized equation can be cast into standard form (See Ref. 1 and 3)

$$a_P \Phi_P = \sum a_{nb} \Phi_{nb} + S_C^\Phi, \qquad a_P = \sum a_{nb} - S_P^\Phi. \quad (9)$$

The implicit numerical dissipation model[1,3,4] is a combination of Rhie-Chow type interpolation for mass flux and a retarded density. It is used to extract the damping mechanism from the second- and fourth-order differencing formulation, which is expressed in pressure for all transport equations. A standard $k - \epsilon$ turbulent closure with a near-wall one-equation model[13] is used for the turbulent flow cases. The calculation starts from uniform flow condition. Boundary conditions everywhere use the same strategy for the Euler and Navier-Stokes equations, except at solid walls where the slip condition is used for Euler and the no-slip conditions for Navier-Stokes. The values of k and ϵ were extrapolated at outlets.

4 Results and Concluding Remarks

The computed results for the inviscid flow around airfoil NACA 0012 are compared with Pulliam and Barton's[14] in Fig 2. The results of the prediction of the turbulent flow around airfoil RAE 2822 for *case* 6, and *case* 10 are shown in Figs 3 and 4. From these results we can conclude that

* An advanced pressure-based method can predict both inviscid and turbulent transonic aerodynamic flows with a satisfactory accuracy comparable to, or better than, time-marching method.
* A new proposed third-order upwinding scheme CHARM (Cubic-parabolic High Accuracy Resolution Method) give better resolution for the present inviscid case than the TVD MUSCL scheme (see Fig.2). The linear (in sense of NVD) QUICK gives an unreasonable solution for this case.
* For the turbulent flow cases, both the third-order scheme CHARM and the second-order schemes HLPA and LUDS yield solutions comparable to QUICK.

References

[1] Zhou, G. Davidson, L. and Olsson E., AIAA paper 94-2345, June, 1994.

[2] Lai, Y. G., So, R.M.C. and Przekwas, A. J., AIAA paper 93-2902, July, 1993.

[3] Zhou, G. and Davidson, L., Submitted to *Journal of Computational Fluid Dynamics*, 1994.

[4] Zhou, G., Davidson, L. and Olsson E., *Report.*, Thermo and Fluid Dynamics, CTH, 1994.

[5] Leonard, B. P., *Comp. Meth. Appl. Mech. Eng.*, Vol. 19, pp. 59, 1979.

[6] Lien, F-S and Leschziner, M. A., *Proc. 5th Int. IAHR Symp. on Refind Flow Modeling and Turbulence Measurements*, Paris, Sept. 1993.

[7] Zhou, G. and Davidson, L., *Report.*, Thermo and Fluid Dynamics, CTH, 1994.

[8] Gaskell, P. H. and Lau, A. K. C., *J. Numer. Methods Fluids*, Vol. 8, pp. 617, 1988.

[9] Leonard, B. P., *Int. J. Numer. Methods Fluids*, Vol. 8, pp. 1291 1988.

[10] Zhu J., *Comp. Meth. Appl. Mech. Eng.*, Vol. 98, pp. 345, 1992.

[11] van Leer., B., *J. Comput. Pyys.,* Vol. 32, pp. 101, 1979.

[12] Cook, P. H., McDonald, M. A., and Firmin, M. C. P., *AGARD Report*, No.138., 1979.

[13] Chen, H. C. and Patel, V. C., AIAA paper 87-1300, June, 1987.

[14] Pulliam, T. H. and Barton, J. T., AIAA paper 85-0018, January, 1985.

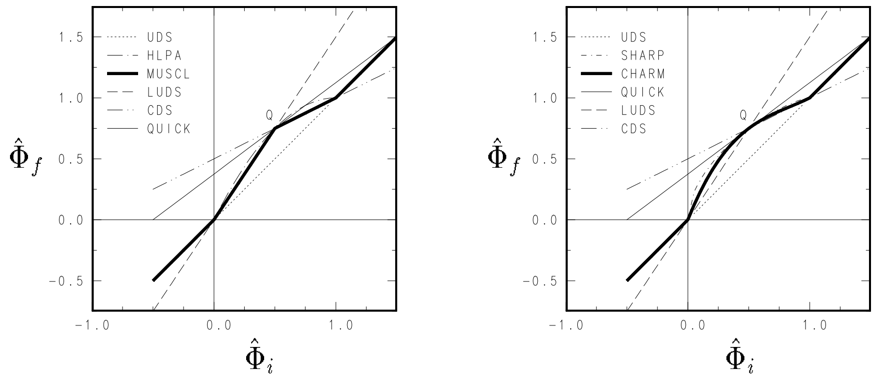

Figure 1. Characteristic of MUSCL (left) and CHARM (right)

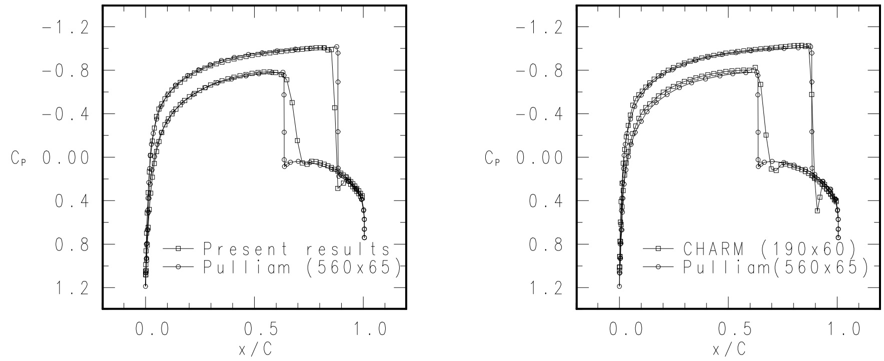

Figure 2. Euler solution for NACA 0012, $M_\infty = 0.85, \alpha = 1.00$, Pressure distribution, from MUSCL (left) and CHARM (right)

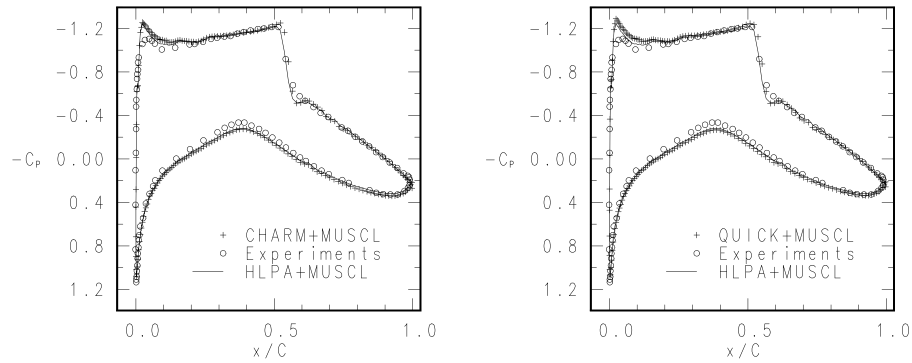

Figure 3. Turbulent N-S solution for RAE 2822, case 6.

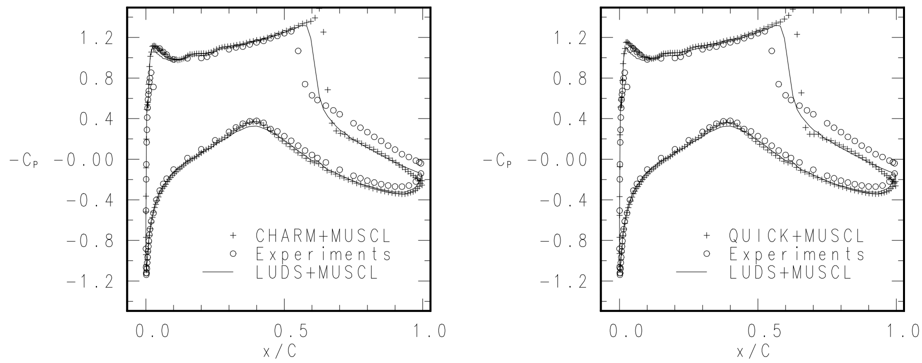

Figure 4. Turbulent N-S solution for RAE 2822, case 10.